JACS
JOURNAL OF THE AMERICAN CHEMICAL SOCIETY
Article
pubs.acs.org/JACS

Biomimetic Crystalline Actuators: Structure–Kinematic Aspects of the Self-Actuation and Motility of Thermosalient Crystals

Subash Chandra Sahoo,[†] Manas K. Panda,[†] Naba K. Nath, and Panče Naumov*

New York University Abu Dhabi, P.O. Box 129188, Abu Dhabi, United Arab Emirates

Supporting Information

ABSTRACT: While self-actuation and motility are habitual for humans and nonsessile animals, they are hardly intuitive for simple, lifeless, homogeneous objects. Among mechanically responsive materials, the few accidentally discovered examples of crystals that when heated suddenly jump, propelling themselves to distances that can reach thousands of times their own size in less than 1 ms, provide the most impressive display of the conversion of heat into mechanical work. Such *thermosalient crystals* are biomimetic, nonpolymeric self-actuators par excellence. Yet, due to the exclusivity and incongruity of the phenomenon, as well as because of the unavailability of ready analytical methodology for its characterization, the reasons behind this colossal self-actuation remain unexplained. Aimed at unraveling the mechanistic aspects of the related processes, herein we establish the first systematic assessment of the interplay among the thermodynamic, kinematic, structural, and macroscopic factors driving the thermosalient phenomenon. The collective results are consistent with a latent but very rapid anisotropic unit cell deformation in a two-stage process that ultimately results in crystal explosion, separation of debris, or crystal reshaping. The structural perturbations point to a mechanism similar to phase transitions of the martensitic family.

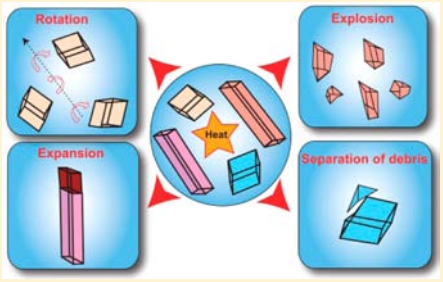

1. INTRODUCTION

Nature has devised mechanisms for active locomotion of plants, typically observed as rapid movements for prey and defense or as very slow movements during growth. Passive motility includes seeds of some plants that snap, buckle, and explode to disperse or to burrow themselves in the soil in response to periodic changes in humidity and/or temperature.[1] When in arid conditions, some grass awns commonly undergo torsional motion for burial. The awns of wheat (*Triticum turgidum*),[2] needle-and-thread grass (*Hesperostipa* sp.),[3] and some *Avena* and *Erodium* species,[4] for instance, are effective drillers that are capable of self-cultivation by propelling themselves into the soil. Other disseminules are capable of migration by reversibly changing their shape and disperse by creeping, crawling, ratcheting, buckling, or slithering.[5−8]

While motility is known with seeds and plant organs, it is hardly intuitive for simple homogeneous objects. Yet, the chemical literature contains sporadic reports of about a dozen crystalline materials that, when heated or cooled, hop on millisecond time scales to leap over distances that, in extreme cases, can reach hundreds or thousands of times their own size (Chart 1).[9−28] Figure 1 shows snapshots of the motions of four such *thermosalient (TS) crystals* captured with a high-speed camera. Bearing in mind that the locomotion of such crystals is strongly alleviated by drag forces due to their small size (μm to mm scale), even stronger effects can be anticipated in the hypothetical absence of the drag. Together with single crystals that bend,[29−52] TS crystals are an invaluable probe into the fast mechanical response of the organic matter under extreme internal pressures and could provide insight into fundamental processes, such as bond cleavage and evolution/migration of phase boundaries at the limits of susceptibility of ordered matter to internal pressure.

Chart 1. Organic-Containing Thermosalient Solids Reported to Date

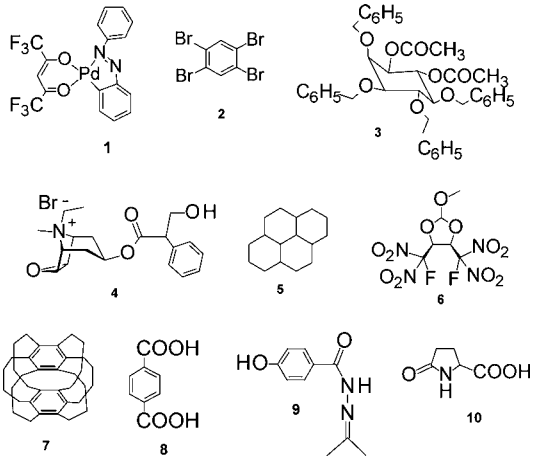

The enduring technical challenges with tracking and analysis of rapid dynamic effects of small objects and the lack of viable mechanistic rationale for the observations have thus far hampered elucidation of the mechanistic details of this visually extraordinary, impressive, and potentially useful phenomenon.

Received: April 27, 2013
Published: July 22, 2013

   dx.doi.org/10.1021/ja404192g | J. Am. Chem. Soc. 2013, 135, 12241−12251

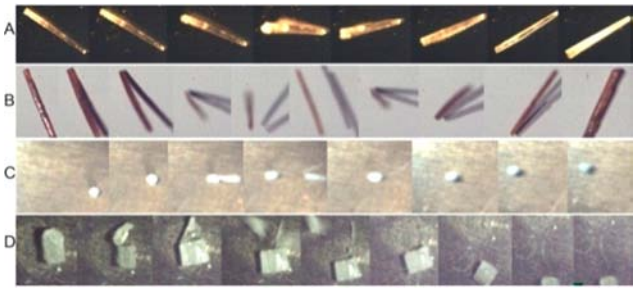

Figure 1. Motility in thermosalient crystals recorded with a high-speed camera: 1,2,4,5-tetrabromobenzene (TBB, **2**; A), (phenylazophenyl)-palladium hexafluoroacetylacetonate (PHA, **1**; B), oxitropium bromide (OXTB, **4**; C), and *N*′-2-propylidene-4-hydroxybenzohydrazide (PHBH, **9**; D). The snapshots were taken at intervals of 1 ms.

Generally, the colossal mechanical response observed with TS crystals indicates that the effect occurs in response to extreme strains that accumulate inside a crystal and are cooperatively released on a very short time scale. Several studies have suggested[12,21,23,28] that the phase transitions responsible for the TS phenomenon could have diffusionless, lattice-distortive character, similar to martensitic phase transitions, although the direct analogy between the TS transitions in organic/metal–organic compounds and the true martensitic transformation in metal alloys remains inconspicuous. Although the scarcity of data has precluded systematic assessment of the kinematic and thermodynamic profiles of TS solids, the thermal data discussed here as well as the readily observable propagation of the product phase in the crystal of **1** (the only colored compound among the TS solids **1**–**10**)[13] seem to support that hypothesis.

Herein, with the first comparative analysis of the TS effect, we set as our goal to elucidate qualitative and semiquantitative correlations among the thermodynamic, structural, and kinematic properties of TS crystals and to decipher any general relationships between the molecular mechanism and the macroscopic manifestation of the phenomenon. For the experimental part, out of about a dozen known TS-active materials in Chart 1 we selected four structurally diverse solids: (phenylazophenyl)palladium hexafluoroacetylacetonate (PHA, **1**),[13] 1,2,4,5-tetrabromobenzene (TBB, **2**),[14] oxitropium bromide (OXTB, **4**),[21,22] and *N*′-2-propylidene-4-hydroxybenzohydrazide (PHBH, **9**).[12] To arrive at more general inferences, we also analyzed the available structural data of all TS compounds reported thus far (Chart 1). The relevant structural parameters were extracted by comparison between the crystal structures of the TS phases.

2. RESULTS

2.1. Thermal Profile of the TS Phenomenon. To unravel the origin of the TS phenomenon, we performed an extensive set of differential scanning calorimetry (DSC) measurements under various conditions and with different samples. Specifically, in multiple experiments we examined the effects of thermal cycling, heating rate, single vs polycrystalline samples, and pretreatment by grinding. The molar enthalpy and temperatures of the forward and the reverse TS transition determined by DSC from hand-selected pristine crystals and ground powdered samples were compared as directly measurable thermodynamic parameters (Table 1).

The DSC of all TS crystals consistently displayed profiles with multiple sharp peaks that appear as a characteristic

Table 1. Thermoanalytical Data for the Four Thermosalient Compounds

	first phase transition		reverse or second phase transition	
sample	θ (°C)	ΔH (kJ mol^{-1})	θ (°C)	ΔH (kJ mol^{-1})
	$\alpha \rightarrow \gamma$		$\gamma \rightarrow \alpha$	
PHA (crystals)[a]	69.1–76.9	1.32	52.7–32.1	−0.735
PHA (powder)[a]	–	–	–	–
	I → II		II → I	
OXTB (crystals)	51.6	3.05	35.7	−3.06
OXTB (powder)	61.1	1.45	28.6[b]	–[c]
	I → II		II → III	
PHBH (crystals)	142.2–149.8	0.712	79.4[b]	−1.32
PHBH (powder)	148.0	0.494	77.9[b]	−1.40
	$\beta \rightarrow \gamma$		$\gamma \rightarrow \beta$	
TBB (crystals)	42.2	0.355	32.7	−0.354
TBB (powder)	~43.0	–	32.8	–

[a]The second, nonthermosalient transition $\gamma \rightarrow \beta$ (orange-to-red) proceeds at $\theta_{\uparrow}$ = 95.7 °C with $\Delta H_{\uparrow}$ = 5.95 kJ mol^{-1} for PHA crystals and $\theta_{\uparrow}$ = 100.3 °C with $\Delta H_{\uparrow}$ = 7.28 kJ mol^{-1} for PHA powder. [b]Nonthermosalient phase transition. [c]Out of the detection limits.

signature of the TS phenomenon in pristine crystals (Figure 2). This sawtooth DSC profile has been previously noted for the

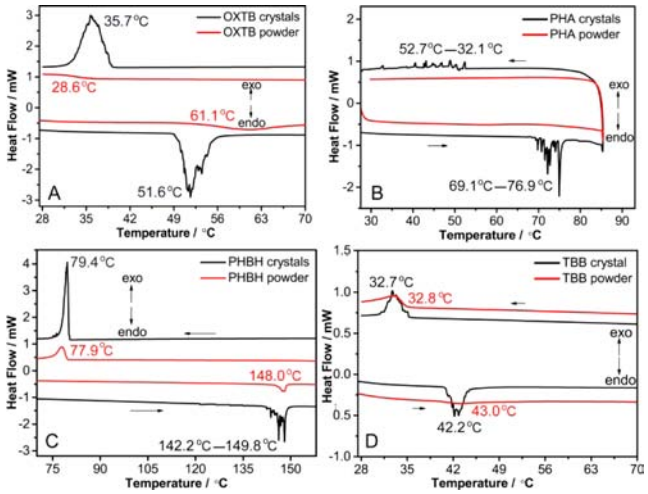

Figure 2. Thermal signature on heating and cooling of crystals (black curve) and powders (red curve) of thermosalient (jumping) solids: oxitropium bromide (OXTB; A), (phenylazophenyl)palladium hexafluoroacetylacetonate (PHA; B), *N*′-2-propylidene-4-hydroxybenzohydrazide (PHBH; C), and 1,2,4,5-tetrabromobenzene (TBB; D).

low-temperature phase transition ($\alpha \rightarrow \alpha'$) of pyroglutamic acid (**10**) and associated with martensitic phase transition,[53] although experimental evidence on its origin has yet to be advanced. A similar profile has also been observed previously in glycine[54] and cysteine[55] and explained as a heterogeneous transformation where different domains are converted at different times. As a typical example, heated (↑) single crystals of OXTB undergo TS phase transition from phase I to phase II

dx.doi.org/10.1021/ja404192g | J. Am. Chem. Soc. 2013, 135, 12241–12251

and jump, and this effect is accompanied by a series of endothermic effects around $\theta_{\uparrow}$ = 51.6 °C (Figure 2A). On cooling (↓), the crystals jump again and revert exothermally to phase I around $\theta_{\downarrow}$ = 35.7 °C. Similarly to OXTB, needle crystals of TBB undergo a TS phase transition $\beta \rightarrow \gamma$ with multiple peaks around $\theta_{\uparrow}$ = 42.2 °C (Figure 2D). This TS transition is reversible, and the $\gamma \rightarrow \beta$ transition occurs at $\theta_{\downarrow}$ = 32.7 °C.

The crystals of the yellow phase (α) of PHA (**1**) contribute illustrative evidence that the sawtooth profile is a common signature of the TS transitions (Figure 2B). On heating from room temperature to 150 °C, the crystals of α-PHA display two consecutive endothermic phase transitions. While the first transition ($\alpha \rightarrow \gamma$) at $\theta_{\uparrow}$ = 69.1−76.9 °C, from orange-yellow phase to a red phase, is TS-active (crystals jump several centimeters) and shows the characteristic sawtooth profile, the second transition ($\gamma \rightarrow \beta$) is not TS-active; it is accompanied by a change of color from red to dark red and appears as a single symmetric peak at $\theta_{\uparrow}$ = 95.7 °C. If the heating is terminated after the intermediate phase (γ) was created and this form is cooled before it converts to form β, the crystals jump again. Correspondingly, the characteristic sawtooth pattern reappears in the range $\theta_{\downarrow}$ = 52.7−32.1 °C ($\gamma \rightarrow \alpha$; Figure 2B). If the sample is thermally cycled below the temperature of the $\gamma \rightarrow \beta$ transition, the effect reoccurs. However, if the form γ phase is converted to the high-temperature phase β at $\theta_{\uparrow}$ = 95.7 °C, the process becomes irreversible—the transition to form α does not occur on cooling to room temperature and the jumping ceases (a transition at lower temperature cannot be excluded).

Similar to PHA, PHBH is also trimorphic. When heated, crystals of form I PHBH undergo TS transition to phase II with jumps that were reported to reach up to 1 m[12] and with characteristic sharp peaks in the range $\theta_{\uparrow}$ = 142.2−149.8 °C (Figure 2C). When cooled, at $\theta_{\downarrow}$ = 79.4 °C form II transforms to another polymorph, form III, the transition is not TS, and the crystals remain still. Owing to this irreversible transformation, crystals of PHBH do not exhibit the sawtooth profile after the first heating−cooling cycle (Figure 2C).

The spiky appearance of the DSC profiles and the temporal resolution of the sharp peaks in the thermal profile observed with the TS solids can be a result of three factors: (1) different *crystals* (that is, crystals of different sizes) in the same sample undergo phase transition at different temperatures, (2) different *domains* of a single TS-active crystal undergo transition at different temperatures, or (3) the peaks observed in the DSC curve are not intrinsic to the phase transition and are solely a result of the mechanical effect where the crystals hopping off the bottom of the pan disturb the heat flow between the sample and the temperature sensor.

The lack of reproducibility of the profile with different samples from the same batch, as well as by thermal cycling of the same sample over the phase transition, indicated that the series of peaks in the DSC profile of the TS transition are not intrinsic to the structural change of the bulk material; instead, they are probably related, directly or indirectly, to the crystal size distribution. The series of peaks could originate from crystals of different sizes undergoing the phase transition at slightly different temperatures and/or from the mechanical effect: the crystals hop off the base or disintegrate at slightly different temperatures, thereby disturbing the heat flow between the sample and the detector. To check this, we recorded DSC curves of several large single crystals of PHA. All crystals exhibited a single peak on heating but multiple peaks in the subsequent cooling run (Figure 3D). The temperature depended strongly on the sample; four crystalline blocks,

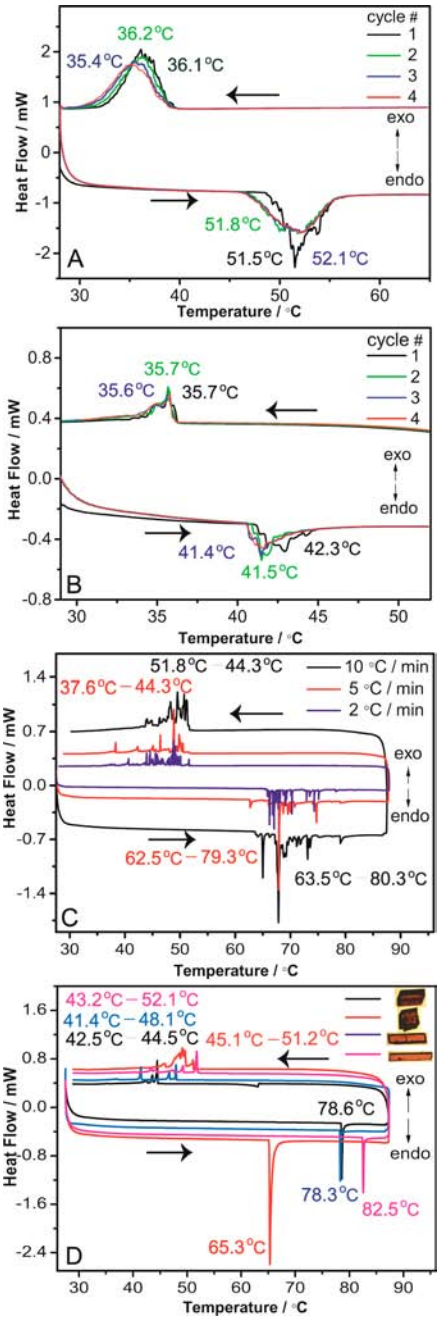

Figure 3. (A and B) Effects of thermal cycling on the thermosalient phase transitions in oxitropium bromide (OXTB, **4**; A) and 1,2,4,5-tetrabromobenzene (TBB, **2**; B). (C) Effect of heating rate on the thermal profile of PHA (**1**). (D) DSC profiles of four PHA crystals (three single crystals) shown in the inset.

including three single crystals and one multiple crystal, underwent a transition at very different temperatures that span a range of 17.2 °C (65.3, 78.3, 78.6, 82.5 °C; Figure 3D). Notably, the crystalline block that was apparently not a single crystal was converted at the lowest temperature (65.3 °C). These results confirm that the multiple peaks in the DSC profile are a result of different crystals undergoing the TS phase transition at different temperatures. Crystals with defects or single crystal multiplets probably undergo phase transition at

dx.doi.org/10.1021/ja404192g | J. Am. Chem. Soc. 2013, 135, 12241−12251

lower temperatures, which is perhaps the reason why the series of DSC peaks of heated samples is oftentimes terminated with a single strong peak (Figure 2B,C) that corresponds to simultaneous conversion of all remaining (nonconverted) single crystals within the sample.

2.2. Effects of Thermal Cycling. In the first set of experiments, polycrystalline samples of two bistable TS solids, OXTB and TBB, with different packing patterns (three-dimensional and layered), were cycled thermally over their TS transitions. The hopping reoccurred, although the jumps became gradually less forceful and were accompanied by fragmentation. The peak profile in the sawtooth section of the thermal curve changed with each cycle, while its contour became progressively smoother (Figure 3A,B), and it also depended on the heating rate (Figure 3C). The gradual smoothing is indicative of progressive crystal disintegration. Since the crystals tend to partially disintegrate, the lack of reproducibility of the profile upon thermal cycling of the sample indicates that it depends on the crystals size distribution. In line with this conclusion, the contour profiles of the TS peaks of different lots of crystals from the same batch were erratic (for multiple samples from a batch of PHA crystals, see Figure 3C). Due to evolution of domains, the thermal cycling is usually related to development of cracks and other surface imperfections on the crystal. This behavior resembles that observed with glycine,[54] cysteine,[55] and paracetamol[56] and can be attributed to Grinfeld surface instability.[57] As a result, the crystals are prone to separation of debris or disintegration.

2.3. Effects of Grinding. During the thermal analysis of the TS solids, we noticed that powdering had a dramatic effect and led to irreversible changes in the DSC behavior. On grinding, the characteristic multiple-peak pattern of the TS solids disappeared, and the intensity of the residual peak as well as the molar enthalpies of the TS-active transitions decreased. In the case of OXTB and PHBH, the TS transition of the ground samples appeared as a much weaker thermal effect with wider hysteresis, while in ground PHA and TBB the transition was almost completely suppressed (Figure 2). OXTB (Figure 2A) provides a typical example of the strong shear-induced effects, where grinding-induced temperature shifts of both forward and reverse transition ($\theta_{\uparrow}$ = 51.6 °C, $\theta_{\downarrow}$ = 35.7 °C to $\theta_{\uparrow}$ = 61.1 °C, $\theta_{\downarrow}$ = 28.6 °C), and the hysteresis gap was nearly doubled ($\Delta\theta$ = 15.9−32.5 °C). Accordingly, grinding had a strong effect on the thermal behavior of PHBH (Figure 2C) and TBB (Figure 2D). In the case of PHA (Figure 2B), the TS transition ($\alpha \rightarrow \gamma$) was completely suppressed by grinding and we could not observe evidence of any thermal effect. The second, non-TS transition ($\gamma \rightarrow \beta$) still occurred, although at higher temperature ($\theta_{\uparrow}$ = 100.3 °C) relative to pristine crystals ($\theta_{\uparrow}$ = 95.7 °C), indicating that the size effect did not affect the second phase transition. Similar effects have been reported with cysteine.[55]

From a mechanistic viewpoint, the alleviation (or inhibition) of the TS effect by grinding lends support to the assumptions that the mechanical actuation in TS crystals occurs in response to internal stress that builds up within the crystal interior. The size of a crystal is known to have a profound effect on the conditions of stress relaxation: crystal fragmentation and even dislocation generation become impossible starting from some critical small size. The critical effect of the history of the sample is in line with some previous conclusions[48−52] based on the Young's modulus that mechanically responsive crystals are generally "soft" media that are highly susceptibility to pressure. Indeed, single TS crystals can withstand a significant amount of internal strain before the phase change is triggered.

On the basis of the thermoanalytical results, it can be suggested that the temperature change induces structural perturbations with a gradual accrual of structural strain. The transition in such strained structure is then triggered, leading to very rapid cooperative long-range molecular change that macroscopically appears as separation of debris, explosion, and/or dislocation of the crystal. Suppression of the transition is effectuated by evolution of quasilatent strains in the microcrystals and/or by particle size reduction. As an important practical inference, in a routine DSC analysis, mechanical effects accompanying a phase transition could easily be overlooked if the sample was subjected to standard grinding preparation procedures;[55] a simultaneous visual inspection and thermoanalytical measurement of nongrinded crystals is critical to detect the occurrence of this phenomenon. This conclusion is in line with the fact that practically all reported cases of jumping crystals were observed accidentally and always by visual inspection of the behavior of heated crystals on a hot stage or with a microscope.

2.4. Kinematic Analysis of the TS Phenomenon. The selection of macroscopic kinematic measurables and quantification of the related parameters turned out to be the most challenging part of the analysis. Because it was not possible to capture the fast crystal motions with an ordinary digital camera (frame rate 30 fps), for macroscopic kinematic analysis we used a high-speed camera (frame rate 10^3 fps, time resolution 1 ms) coupled with a reflection-mode optical stereomicroscope. This setup was combined with a hot plate for uniform heating and a pointy heating element affixed to an XYZ-stage for localized (nonuniform) heating. To inspect the motility of the crystals, each crystal out of a total of about 150 specimens was individually heated, and their trajectory was examined using tracking software. The comparison of the kinematic behavior of the four TS compounds shows that the thermomechanical response from TBB crystals depends strongly on the heating mode (uniform or localized) and that the deformations are reversible. We also noticed that crystals of PHA exhibit a different kinematic profile relative to the other three materials. The dominating effect was expansion of the crystal along the longest axis, while other kinematic effects were less frequently observed.

The crystals of PHBH (**9**) and OXTB (**4**) were grouped in batches according to their metrics, and the type of mechanical effect was correlated with the crystal length (l), width (w), height (h), and volume (V; see Figures 4 and 5). To account for the natural crystal size distribution, the *relative* number of crystals in a particular size range that undergo a particular effect was calculated as the number of crystals that undergo that effect divided by the total number of crystals within that size range.

Figure 1 shows exemplary snapshots from the high-speed recordings, and Table 3 contains the relevant kinematic information. Detailed analysis of the recorded material [for examples, see Movies S1−S8, Supporting Information (SI)] showed that kinematically the TS phenomenon is a nonuniform effect that occurs as several events. On the basis of individual inspection of the motion behavior of each crystal, we classified the trajectories of the hopping crystals into different effects. For kinematic analysis of PHBH, which crystallizes as transparent blocks (Figure 1D), over 35 crystals were selected and analyzed (Figure 4). With PHBH crystals, we observed four types of mechanical effects: crystal explosion (effect 1), rotation

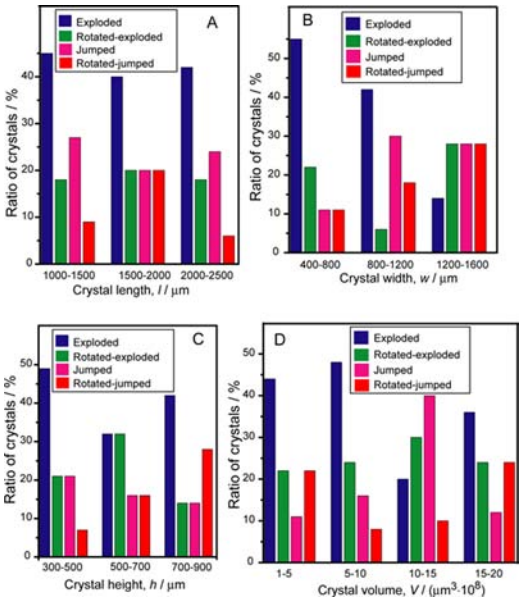

Figure 4. Distribution of kinematic effects of crystals of PHBH over the crystal size.

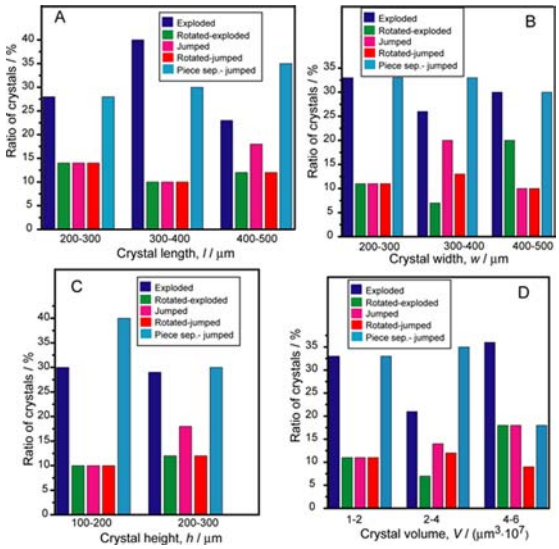

Figure 5. Distribution of kinematic effects of crystals of OXTB over the crystal size.

followed by a steady period and delayed explosion (effect 2), hopping (effect 3), and rotation followed by delayed jumping (effect 4). The most frequent manifestation of the TS effect in PHBH was explosion of the crystals (effect 1). We could not observe significant dependence of the ratio of crystals undergoing a certain effect on the crystal axes and volume, except in the case of the dominant effect 1, where the effect occurs preferentially for narrower crystals (w = 400−800 μm) and becomes less probable for wider crystals (Figure 4B). Notably, the motions of the crystals of PHBH are on average faster than those of the other three TS compounds, and the actuated crystals can reach longer distances. With some crystals of PHBH we observed an intriguing kinematic pattern: the crystals were initially rotated, and after settling and remaining still for 2−3 s, they suddenly hopped or exploded. The initial rotation was much slower than the hopping/explosion. This behavior qualitatively resembles the two-stage mechanism described above. In the first stage, the crystals accumulate stress, and some of them are rotated. In the second stage, additional latent stress accrues in the crystals, while they remain still. Above a certain threshold, the structure switches to the new phase, whereby the stress is released by disintegration or reshaping.

Crystals of OXTB respond mechanically to heat in a similar way as PHBH. OXTB crystals undergo a variety of kinematic effects, including two or three types of complex motions, where the individual movements are separated by a hiatus of several seconds where the crystals remain still. We observed five types of mechanical effects: explosion (effect 1), rotation followed by a delayed explosion (effect 2), hopping (effect 3), rotation followed by delayed jumping (effect 4), and separation of debris followed by jumping (effect 5). Effects 1 and 5 were most frequently observed (Figure 5). Effect 5 was also apparent with TBB crystals; however, the crystals of OXTB moved faster. In fact, the locomotion of OXTB crystals was also notably faster relative to that of TBB and PHA. Similar to PHBH, with OXTB we could not observe a clear trend in the distribution of the effects with crystal size.

3. DISCUSSION

3.1. Structural Correlations. The packing of the two polymorphs of TBB, OXTB, and PHBH that are directly involved in the TS transition, analyzed with XPac,[58,59] is very similar. In fact, the structural similarity between the phases that are related through a TS phase transition appears to be more general. As shown in Table 2, which lists the basic structural data for the known TS transitions, except for the two inorganic TS solids (spinels) that undergo cubic-to-tetragonal phase transition driven by cooperative Jahn−Teller effect,[61−63] the crystal symmetry is preserved in all cases. Compared to non-TS phase transitions, the relative cell volume expansion that ranges between +0.7% (**10**) and +4.3% (**9**) is not exceptional.

There are however structural traits that are common for all TS solids. First, most of the crystals undergo remarkable expansion along one or two axes. Second, the expansion is always anisotropic; the expansion along one or two axes [between 0.7% (**10**) and +20.6% (**8**)] is balanced by shrinking along other axes [between −3.1% (**2**) and −25.3% (**8**)].[64,65] We conclude that instead of large overall cell expansion, the required (although probably not sufficient) factor to elicit a strong mechanical response is *anisotropic* cell change; the crystal structure expands preferentially in some directions, while shrinking in other directions. In effect, the mass within the cell is effectively redistributed, without substantial overall volume expansion.

Multiphase solids that are capable of both TS-active and TS-nonactive transitions provide a more direct comparative way to determine the factors that drive the TS effect, because the same molecule switches between TS-active and TS-nonactive environments. Only three out of a dozen known TS compounds in Chart 1 undergo multiple phase transitions [PHA (**1**), PHBH (**9**) and pyroglutamic acid (**10**)], but only in the case of PHBH have all phases been structurally characterized.[12] Gratifyingly, the three reported forms of PHBH are orthorhombic with one-to-one correspondence of their unit cell axes, and thus, their molecular packing motifs are directly comparable. In the course of this work, we obtained a new, fourth (monoclinic) polymorph of PHBH[66] (for complete crystallographic details, see Table S1 in the SI).

dx.doi.org/10.1021/ja404192g | J. Am. Chem. Soc. 2013, 135, 12241−12251

Table 2. Literature Data on Temperatures of the Phase Transitions (θ) and Change of the Basic Crystallographic Parameters of Thermosalient Crystals[a]

	phase	θ/°C transition	θ/°C structure	system	SG	a/Å	b/Å	c/Å	α/deg	β/deg	γ/deg	(V/Z)/Å^3	ρ/(g·cm^{-3})	Z
						Organic and Metal–Organic Crystals								
1[b]	LT	90(10)	RT	triclinic	$P\bar{1}$	13.205(3)	15.715(3)	8.436(3)	93.61(2)	86.98(2)	95.40(2)	434	1.90	4
	HT[b]		RT	triclinic	$P\bar{1}$	11.677(2)	12.465(2)	6.992(3)	95.20(2)	63.11(1)	98.80(2)	448	1.84	2
	Δ/%					−11.6	−20.7	−17.1	+1.7	−27.4	+3.6	+3.2	−3.2	
2[c]	LT	45.5	RT	monoclinic	$P2_1/a$	10.323(1)	10.705(1)	4.018(4)	90	102.4(1)	90	217	3.015	2
	HT		69(5)	monoclinic	$P2_1/a$	10.00(1)	11.18(1)	4.07(2)	90	103.8(4)	90	221	2.957	2
	Δ/%					−3.1	+4.4	+1.3	0	+1.4	0	+1.8	−2.0	
3[d]	LT[e]	70/40	60	monoclinic	$P2_1/c$	14.464(6)	14.923(5)	16.385(6)	90	102.73(3)	90	862	1.203	4
	HT		80	monoclinic	$P2_1/c$	16.261(8)	15.230(8)	14.385(7)	90	96.73(4)	90	883	1.173	4
	Δ/%					+12.4	+2.0	−12.2	0	−5.8	0	+2.4	−2.5	
4[f]	LT	45/27	23	orthorhombic	$P2_12_12_1$	7.3927(2)	10.1512(4)	24.6291(9)	90	90	90	462	1.482	4
	HT		29	orthorhombic	$P2_12_12_1$	7.453(3)	11.220(4)	22.790(7)	90	90	90	476	1.437	4
	Δ/%					+0.8	+10.5	−7.5	0	0	0	+3.0	−3.0	
5[g]	LT	71.5/65.5	RT	monoclinic	$P2_1/c$	16.782(7)	5.447(1)	16.710(7)	90	120.00(3)	90	331	1.097	4
6[h]	LT	40	−100	monoclinic	$C2/c$	17.816(2)	9.0500(10)	15.468(3)	90	98.700(10)	90	308	1.876	8
7[i]	LT	>300	−180	orthorhombic	$Cmca$	15.471(9)	11.435(7)	11.325(4)	90	90	90	500	1.315	4
8[j,k]	II	75–100	RT	triclinic	$P\bar{1}$	9.54(1)	5.34(1)	5.02(1)	86.95(5)	134.65(5)	104.90(5)	173	1.597	1
	I	>30	RT	triclinic	$P\bar{1}$	7.730	6.443	3.749	92.75	109.15	95.95	175	1.579	1
	Δ/%					−20.0	+20.6	−25.3	+6.7	−18.9	−8.5	+1.1	−1.1	
9[l]	I	147	20	orthorhombic	$Pna2_1$	9.157(4)	7.196(3)	15.566(6)	90	90	90	256	1.245	4
	II	80[m]	95	orthorhombic	$Pna2_1$	9.968(5)	8.082(5)	13.267(8)	90	90	90	267	1.195	4
	Δ/%					+8.8	+12.3	−14.8	0	0	0	+4.3	−4.0	
10[n]	α	68/54[o,p]	40[q]	orthorhombic	$P2_12_12_1$	8.964(4)	13.349(6)	14.49(1)	90	90	90	144	–	12
	β		80	orthorhombic	$P2_12_12_1$	9.086(6)	13.140(6)	14.586(7)	90	90	90	145	–	12
	Δ/%					+1.4	−1.6	+0.7	0	0	0	+0.7	–	
						Inorganic Crystals								
11[r]	LT	47/?	25	tetragonal	$I4_1/amd$	5.8369(4)	5.8369(4)	8.4301(6)	90	90	90	72	–	4
	HT		80	cubic	$Fd\bar{3}m$	8.3155(7)	8.3155(7)	8.3155(7)	90	90	90	72	–	8

dx.doi.org/10.1021/ja404192g | J. Am. Chem. Soc. 2013, 135, 12241−12251

Table 2. continued

	phase	θ/°C transition	θ/°C structure	system	SG	a/Å	b/Å	c/Å	α/deg	β/deg	γ/deg	(V/Z)/Å^3	ρ/(g·cm^{-3})	Z
	Δ/%					+42.5	+42.5	−1.3	0	0	0	+0.1	–	
Inorganic Crystals														
12[s]	LT	581/?	567	tetragonal	$I4_1/amd$	6.016(4)	6.016(4)	7.981(4)	90	90	90	72	–	4
	HT		582	cubic	$Fd\bar{3}m$	8.344(2)	8.344(2)	8.344(2)	90	90	90	73	–	8
	Δ/%					+38.7	+38.7	+38.7	0	0	0	+0.6	–	

[a]In calculation of the relative changes Δ, a one-to-one correspondence in the cell parameters between the low-temperature (LT) phase and the high-temperature (HT) phase was assumed. This assumption may not be appropriate in some cases because of the different relation between the two cells (for instance, Z of the LT and HT phases in **1** are 2:1; i.e., the cell of the HT phase is half that of the RT phase). [b]**1** = (phenylazophenyl)palladium hexafluoroacetylacetonate.[13] Note that the structure of the high-temperature phase does not correspond to the phase involved in the TS transition. [c]**2** = 1,2,4,5-tetrabromobenzene.[14] [d]**3** = (±)-3,4-di-*O*-acetyl-1,2,5,6-tetra-*O*-benzyl-*myo*-inositol.[18] [e]These data refer to the structure at 60 °C. The parameters of the same phase at 18 °C are a = 14.269(2) Å, b = 14.862(2) Å, c = 16.506(3) Å, β = 103.21(1)°, V = 3407(1) Å^3, Z = 4. The LT phase of the compound undergoes another phase transition at lower temperature (at 30 and 11 °C on heating and cooling, respectively). [f]**4** = Oxitropium bromide.[22] [g]**5** = *trans,trans,anti,trans,trans*-perhydropyrene.[23] [h]**6** = 4,5-bis(fluorodinitromethyl)-2-methoxy-1,3-dioxolane.[24] [i]**7** = [3$_6$](1,2,3,4,5,6)cyclophane (Yasutake, M.; Sakamoto, Y.; Onaka, S.; Sako, K.; Tatemitsu, H.; Shinmyozu, T. *Tetrahedron Lett.* **2000**, *41*, 7933). [j]**8** = Terephthalic acid.[25] [k]A monoclinic polymorph was also reported: Śledź, M.; Janczak, J.; Kubiak, R. *J. Mol. Struct.* **2001**, *595*, 77. [l]**9** = *N*′-2-propylidene-4-hydroxybenzohydrazide.[12] [m]Transforms into another phase, phase III. [n]**10** = pyroglutamic acid.[53] [o]Reference 28. [p]Reference 53. [q]For additional crystallographic data [a = 9.018(8) Å, b = 13.495(8) Å, c = 14.662(4) Å, V = 1784 Å^3, Z = 12] on the α phase, see the work of Kroon et al.[60] [r]**11** = Nickel(II) chromite, $NiCr_2O_4$. [61] [s]**12** = Copper(II) chromite, $CuCr_2O_4$.[61]

In line with the above conclusions that the cell expansion is an insufficient condition for occurrence of the TS effect, the cell of PHBH expands on heating with similar relative changes in the cell volume and density, irrespective of whether the transition is TS-active (I → II) or not (III → II) (Table 4). Comparative analysis of the crystal packing of the four forms with XPac[58,59] (see Figures S1 and S2 in the SI) indicates the following order of decreasing similarity: II/III > III/IV > I/II > I/III, I/IV, II/IV. Figure 6 illustrates gradual changes in the packing structure, and Table 4 shows the expansion and contraction of the unit cell on going from form I to form III (form IV is monoclinic and has a very different packing). The polymorph pairs I/II and III/IV are one-dimensional isostructural[67] with a 1D supramolecular construct[58,59] and dissimilarity index[68] X = 14.4 (I/II) and 7.7 (III/IV). The pair II/III is two-dimensional isostructural, with a 2D supramolecular construct and X = 11.8. The value of the unit cell similarity index[69] (Π) shows greater similarity of the pairs I/II (Π = 0.019) and II/III (Π = 0.025) relative to pair I/III (Π = 0.044). XPac does not indicate any significant structural similarities for the structure pairs I/III, I/IV, and II/IV.

3.2. Mechanistic Considerations. Why do some crystals jump? Generally, self-actuation of a still object can be triggered by (1) a sudden and strong deformation of the object or (2) a ballistic event where a rapidly leaving entity transfers momentum to the object in accordance with Newton's third law of motion. Careful inspection of the high-speed recordings (resolution 1 ms) of a number of different TS crystals revealed that the separation of debris or explosion are the primary driving forces behind their self-actuation (Figure 1). The second common effect is reshaping of crystals. Crystals that incorporate extensive hydrogen-bonded networks, such as the terephthalic acid,[25] can be taken over the phase transition without mechanical deformation. However, rapid shape changes can easily be induced in such metastable state by local mechanical stimulation (e.g., by poking the crystal with a sharp metal object). Such low-dimensional hydrogen-bonded-network structures are apparently capable of additional storage of latent strain; the phase transformation is stalled and can be triggered by applying local pressure. More extended hydrogen-bonding networks are expected to absorb and channel the release of strain, thereby inhibiting the TS effect. Accordingly, TS effect is not observed with structures having three-dimensional hydrogen-bonded networks. Moreover, latency in the expression of the mechanical effect is not observed with TS architectures having bulky substituents that lack extended bonded networks [for example, OXTB (**4**)].

Our kinematic assessment indicates that the difference between the two TS modes (separation of debris and reshaping) depends, inter alia, on crystal multiplicity. In a recent study of a photoinduced analogue of the TS effect in a photoreactive hydroxybenzylidenedimethylimidazolinone, we found that while hopping of single crystals occurred by partial disintegration (splitting, separation of debris, or explosion), thin crystals were actuated by reshaping without any apparent splitting or separation of debris.[36] A viable explanation for this observation is that multiple crystals are capable of absorbing at their twinning interface(s) additional strain that evolves from structural misfits during the phase transition of their parts, and thus, they jump as a result of fast reshaping instead of explosion. This conclusion is in line with the softness of the TS-active crystals. Additional support is provided by acicular crystals of TBB ($\theta_{transition}$ = 46 °C), which are the only almost

Table 3. Kinematic Parameters for the TS Solids 1, 2, 4, and 9

parameter	PHA (1)	OXTB (4)	PHBH (9)	TBB (2)
θ/°C[a]	69−83.5	51.6	142−149.8	46
N[b]	10	12	14	13
m_{ave}/kg	1.702×10^{-7}	5.186×10^{-8}	1.263×10^{-6}	2.271×10^{-6}
V_{ave}/m^3	9.428×10^{-11}	3.609×10^{-11}	1.014×10^{-9}	7.391×10^{-10}
t_{ave}/s[c]	0.028	0.018	0.020	0.022
v_{xy} /(ms^{-1})[d]	0.021	0.308	0.793	0.230
E_{kxy}/J[e]	3.65×10^{-11}	3.641×10^{-9}	7.397×10^{-7}	8.8768×10^{-8}

[a]Temperature of the phase transition on heating. [b]Number of crystals from which the average speed was calculated. [c]Time of flight. [d]Velocity of the projected trajectory on the 2D microscopic field. [e]*xy*-component of the kinetic energy.

Table 4. Basic Structural Data for Three of the Four Polymorphs and Phase Transitions of *N*′-2-Propylidene-4-hydroxybenzohydrazide (PHBH, 9)[12]

	thermosalient transition			nonthermosalient transition		no thermal phase transition
	phase I	Δ(I→II)/%	phase II	Δ(III→II)/%	phase III	Δ(I and III)/%
a/Å	9.157(4)	+8.9	9.968(5)	+0.9	9.875(2)	+7.8
b/Å	7.196(3)	+12.3	8.082(5)	−11.2	9.103(3)	+26.5
c/Å	15.566(6)	−14.8	13.267(8)	+14.5	11.590(5)	−25.5
V/Å^3	1025.7(7)	+4.2	1069(1)	+2.6	1041.8(6)	+1.6
ρ/(g cm^{-3})	1.245	−4.0	1.195	−2.4	1.225	−1.6
θ/°C	20		95		20	

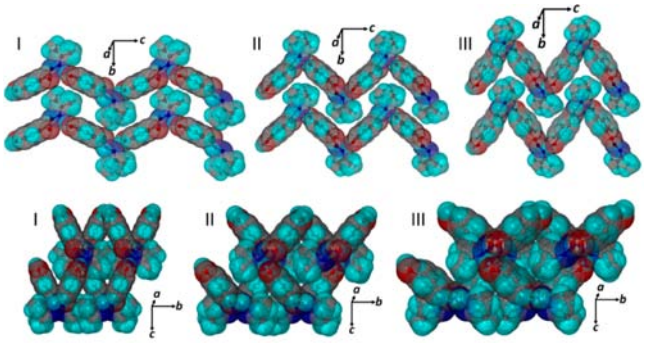

Figure 6. Two views of the stepwise contraction of the crystal lattice along *c* (top) and stepwise expansion along *b* (bottom) in the three polymorphs of PHBH. The crystallographic data were retrieved from a paper by Centore et al.[12]

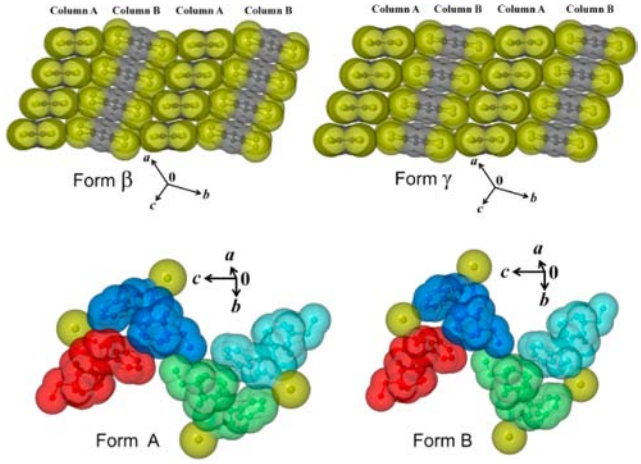

Figure 7. Structural changes of class I (TBB, top) and class II (OXTB, bottom) organic martensites. In the lower plots, four molecules are color-coded for clarity. The contraction along the *c* axis, assessed through the centroid-to-centroid distance between the molecules in red and blue, is from 18.699 Å (form A) to 17.815 Å (form B). Similarly, the cell expands along *b*, assessed from the separation between the molecules in blue and red (or light blue and green) colors, from 7.785 Å (form A) to 8.201 Å (form B). The crystallographic data were retrieved from ref 14 (Davey et al.) and ref 22 (Naumov, Bernstein et al.).

Figure 8. Induction of undulation motions along a crystal twin of TBB by periodic lateral heating (in this figure, the heater is visible on the top right). Note the reversible undulation that can be sustained by approaching the crystal with the heater, as seen by migration of the reflective front marked with red arrows (for details, see Movie S9, SI).

exclusively twinned (twinning ratio >95%) crystals among the known TS compounds. If acicular crystal twins of TBB affixed to a base at one end are heated laterally, they display readily visible undulation motion, as observed by shifting of the alternating light-reflecting bright and dark domains along the crystal under polarized light (Figure 8). These crystal undulations can be induced continually by periodic approaching and retraction of a pointy heater from the crystal. If the crystal is heated above a critical temperature, where the supplied kinetic energy overcomes the threshold in the contact lattice energy, the crystal eventually splits along the twinning axis. Further heating of the partially split twin induces a scissoring motion—the two crystals components oscillate by seceding and rejoining.

On several occasions,[12,21,23,28] the thermosalient effect has been related to martensitic-type transitions.[70] Martensitic phase transitions are first-order displacive solid−solid transitions that proceed with homogeneous lattice deformation and without atom diffusion.[71−77] The structural transformation occurs by movement of the habit plane (the plane between the parent and the product phase) induced by small cooperative movement of the atoms, while the overall chemical composition and atomic order are conserved. The packing

dx.doi.org/10.1021/ja404192g | J. Am. Chem. Soc. 2013, 135, 12241−12251

structures of TS systems where the structures of both phases have been determined (Table 2) do not appear to indicate any atypical structural disparity between the polymorphs related through the TS phase transition. This observation discredits a large difference in the *stationary* structures before and after the transition as prerequisite for occurrence of the TS effect. During the TS phase transitions, the individual molecules do not undergo large conformational changes, structural rearrangements, or isolated dislocation relative to the surrounding molecules, consistent with a diffusionless transition. The motions appear to be cooperative in nature, and the distances between groups of structural units are changed in preferred directions within larger domains, as suggested by the thermoanalytical data. Moreover, the TS phase transitions are sharp and hysteretic, and they are associated with marked anisotropy in the unit cell change (Table 2). The mechanical response also occurs during the reverse transition. These generic characteristics are analogous to diffusionless, lattice-distortive phase transitions observed with martensitic alloys.[71−77] The preservation of crystal symmetry, anisotropy in the distortion, large mechanical response with small structural changes, and the characteristic sawtooth profile altogether support the hypothesis that the TS solids can be considered a new example of the *organic-based analogues of martensitic materials*. To be confirmed, this hypothesis requires further proof by detailed study of the kinetics of accumulation of the product phase during the transition, as well as of the formation and spatial propagation of the transformed domains.

3.3. Kinetic Considerations. The occurrence of strong mechanical response despite the similarity between the initial and the final structures indicates evolution and relaxation of structurally dissimilar transient structures/phases, and thus, *dynamic factors* could act as the primary driving force of the TS effect. The effect might be due to larger than usual accumulated strain and/or to rapid release of strain accrued during the structure transition by fast molecular rearrangement. The possibility of external mechanical induction of the crystal reshaping (e.g., by poking of the crystal with sharp object) observed with some sluggish phase transitions;[25] see above) indicates that the fast rate at which the rearrangement occurs is a more viable promoter of the mechanical response. The assumption of fast conversion poses further questions as to whether the mechanism of the spatial progression of the evolving phase is sequential or concerted, that is, whether the transformation advances throughout the crystal in a timely manner or occurs by simultaneous, collective molecular conformational switching within a certain domain. The DSC data are in support of the latter hypothesis.

4. CONCLUSIONS

In summary, we report herein a collection of thermoanalytical, kinematic, and structural evidence for several TS materials. For the first time, we combined the experimental thermodynamic profile of four TS materials with analysis of their kinematic behavior and structures in different solid-state forms to arrive at an explanation of the conditions for occurrence of their self-actuation and motility. To support our conclusions, we also performed systematic analysis on the structure of all TS crystals reported thus far.

The TS phenomenon is a kinematically complex, two-stage process that occurs as five or six kinematic effects. It is fueled by a latent, sudden, and rapid phase transition related by small but anisotropic cell expansion in crystals that are devoid of a strong three-dimensional hydrogen-bonding network. First, a small structural transformation occurs whereby sufficient internal strain is accumulated, and the crystal is prestressed by buildup of internal pressure. Second, the strain is released by rapid structural transformation, resulting in crystal displacement. This is supported by the observation of a two-stage kinematic behavior with some of the crystals described here. In qualitative support of these considerations, acoustic spectra recorded from a heated single crystal of OXTB show two sets of acoustic signals.[22] Either process in this two-stage mechanism poses conditions for occurrence (or absence) of the effect. According to the above discussion, the first event (crystal prestressing) is a necessary but insufficient condition for a mechanical response. The time scale on which the strain is released in the second stage (fast process) is critical to trigger self-actuation. Indeed, a mechanical response will occur only if the strain is released within a very short time interval. Slow or gradual release of the accumulated strain translates into slow resizing/reshaping, deformation, or disintegration of the crystal devoid of notable kinematic effect and displacement. As discussed above, the structural similarity between the phases suggests that the TS crystals pass through highly perturbed structural intermediate(s). After the packing switches to the new phase, the molecules relax to a conformation that is similar to the initial conformation.

In an attempt to correlate the structures with the mechanical effect, we employed the results from the analysis of the packing in the TS materials in Chart 1 (see above) to draw more general mechanistic conclusions based on the molecular shape and potential of these molecules for intermolecular interactions. The detailed comparison of structural, thermodynamic, and kinematic aspects of the known TS materials allows us to categorize them into three classes.

Class I: This group includes flat, rigid molecules that pack in layers (**1**, **2**, **5**, and **7**). A consistent feature of these molecules is the *absence of extended hydrogen bonds*; the molecules are devoid of groups capable of strong intermolecular hydrogen bonding. These considerations indicate that the environment of all-weak intermolecular interactions is required to induce large molecular displacements during the structural transition in this group. Strong intermolecular interactions will absorb the strain in the crystal caused by anisotropic distortion, dampen the molecular displacement, and ultimately suppress the mechanical response.

Class II: This class contains bulky, flexible molecules decorated with multiple substituents on a central core (**3**, **4**, and **6**; note that the hydroxyl group in **4** is engaged in a strong intramolecular hydrogen bond and thus it is effectively unavailable for intermolecular hydrogen bonding). The potential hydrogen-bonding sites in these molecules are sterically hindered for strong intermolecular interactions by bulky groups.

Class III: This group contains molecules that saturate their hydrogen-bonding potential by dimerization or polymerization (**8**−**10**). The phase transitions in this class of materials are sluggish. The pyroglutamic acid (**10**) forms the typical symmetric dicarboxylic dimers. Form II terephthalic acid (**8**), on the other hand, consists of sheets of polymeric, doubly hydrogen-bonded molecules. In both cases, the suggested mechanism is a collective sliding of the hydrogen-bonded assemblies atop each other. The extended hydrogen-bonding network of **8** is the most probable reason for crystal deformation instead of jumping by mechanical stimulation.

The lot of structures of TS materials (Table 2) and their thermodynamic, kinematic, and structural data indicate two main mechanisms for the TS phenomenon. Crystals of class I and III are layered structures of flat molecules connected within the layers by very weak interactions with significant anisotropy in their packing. Heating of these crystals does not excite the major conformational degrees of freedom such as rotations. Instead, the anisotropic distortion upon heating or cooling induces strain that is steadily accumulated within the layers to the point where it ultimately outweighs the cohesive weak interactions between the layers, triggering rapid sliding of the layers. Because of the pronounced structural anisotropy in these crystals, the sliding is reflected in an anisotropic change of the unit cell. The small conformational flexibility renders such structures prone to twinning during the phase transition.

The TS crystals of class II are flexible and have much higher degree of conformational freedom. Thus, heating induces more prominent conformational changes, such as torsion of the molecule and/or rotation of the terminal groups, whereby strain accrues up to the point of the phase transition. At the transition, the molecular packing rapidly switches to the second phase with increased distance between the molecules while their relative orientation is preserved. The new molecular packing accommodates the new conformation better, thereby alleviating the strain. As the new unit cell is less dense, the flexible molecules relax to their energetically most stable conformation, which is usually close to the original conformation. Accordingly, instead of twinning, in their post-TS phases class II organic martensitic crystals typically show increased conformational disorder of their terminal groups.

5. EXPERIMENTAL AND THEORETICAL METHODS

5.1. Materials. PHA (**1**) and PHBH (**9**) were synthesized using reported procedures.[12,13] Commercially available 1,2,4,5-tetrabromobenzene (**2**) (Aldrich) was recrystallized from toluene. Oxitropium bromide (OXTB, **4**) was purchased from the European Directorate for the Quality of Medicines and Health Care (EDQM) and used as received.

5.2. Thermal Analysis. Differential scanning calorimetry (DSC) analyses of the crystals and powder were carried out on TA DSC-Q2000 instrument, using ca. 2−6 mg of the samples. The samples were placed on a Tzero aluminum pan and heated from room temperature to the selected temperature with a heating rate of 10 °C/min. An empty Tzero aluminum pan was used as a reference and the chamber was purged with nitrogen during the experiment.

5.3. Hot-Stage Microscopy. Hot-stage microscopic measurements were performed with a Linkam system that includes a temperature-controlled stage THMS600-PS mounted on a Q-imaging (Q32643) microscope.

5.4. Kinematic Analysis. For digital recordings, an ordinary digital camera and a high-speed camera (HS1280CC) were coupled to a reflectivity-mode optical microscope (Nikon SMZ7451). A hot plate with attached thermocouple was used for uniform heating of the sample. For localized heating, AC current was passed through a thin metal wire mounted on an XYZ micromanipulator stage.

5.5. Analysis of the Crystal Packing. The XPac method[58,59] allows identification of similar packing arrangements in two or more given crystal structures and produces parameters that characterize their degree of similarity, that is, the dissimilarity index (X).[68] The dissimilarity index X is calculated as $X = \sum(\delta_{ai}^2 + \delta_{pi}^2)^{1/2}$, where δ_{ai} and δ_{pi} are the angular parameters for the ith data point. The unit cell similarity index (Π)[69] is defined as

$$\Pi = \left| \frac{a + b + c}{a' + b' + c'} \right| - 1 \cong 0$$

where a, b, c and a', b', c' are orthogonalized lattice parameters of the related structures. For a pair of completely isostructural crystals, Π should be close to zero.

■ ASSOCIATED CONTENT

Supporting Information

Movies of crystal motions recorded with a high-speed camera (Movies S1−S8) and undulation of a TBB crystal recorded with an ordinary digital camera (Movie S9), crystal structure plots (Figures S1 and S2), and crystallographic details for polymorph IV of PHBH (Table S1). This material is available free of charge via the Internet at http://pubs.acs.org.

■ AUTHOR INFORMATION

Corresponding Author

pance.naumov@nyu.edu; phone: +971-(0)2-628-4572; fax: +971-(0)2-628-8616.

Author Contributions

†These authors contributed equally to this study.

Notes

The authors declare no competing financial interest.

■ ACKNOWLEDGMENTS

This study was financially supported by NYU Abu Dhabi. We thank Mrs. Jane Toye for editing the manuscript.

■ REFERENCES

(1) van der Pijl, L. *Principles of Dispersal in Higher Plants*; Springer-Verlag: New York, 1982.
(2) Elbaum, R.; Zaltzman, L.; Burger, I.; Fratzl, P. *Science* **2007**, *316*, 884.
(3) Murbach, L. *Bot. Gaz.* **1990**, *30*, 113.
(4) Stamp, N. E. *Am. J. Bot.* **1989**, *76*, 555.
(5) Kulić, I. M.; Mani, M.; Mohrbach, H.; Thaokar, R.; Mahadevan, L. *Proc. R. Soc. B* **2009**, *276*, 2243.
(6) Armon, S.; Efrati, E.; Kupferman, R.; Sharon, E. *Science* **2011**, *333*, 1726.
(7) Forterre, Y.; Skotheim, J. M.; Dumais, J.; Mahadevan, L. *Nature* **2005**, *433*, 421.
(8) Weintraub, M. *New Phytol.* **1952**, *50*, 357.
(9) Dunitz, J. D.; Bernstein, J. *Acc. Chem. Res.* **1995**, *28*, 193.
(10) Bernstein, J. *Polymorphism in Molecular Crystals*; Oxford University Press: Oxford, 2002; p 223.
(11) Gigg, J.; Gigg, R.; Payne, S.; Conant, R. *J. Chem. Soc., Perkin Trans. 1* **1987**, 2411.
(12) Centore, R.; Jazbinsek, M.; Tuzi, A.; Roviello, A.; Capobianco, A.; Peluso, A. *CrystEngComm* **2012**, *14*, 2645.
(13) Etter, M. C.; Siedle, A. R. *J. Am. Chem. Soc.* **1983**, *105*, 641.
(14) Lieberman, H. F.; Davey, R. J.; Newsham, D. M. *Chem. Mater.* **2000**, *12*, 490.
(15) Trommsdorff, H. *Ann. Chem. Pharm.* **1834**, 190.
(16) Natarajan, A.; Tsai, C. K.; Khan, S. I.; McCarren, P.; Garcia-Garibay, M. A. *J. Am. Chem. Soc.* **2007**, *129*, 9846.
(17) Steiner, T.; Hinrichs, W.; Gigg, R.; Saenger, W. *Z. Kristallogr.* **1988**, *182*, 252.
(18) Steiner, T.; Hinrichs, W.; Saenger, W.; Gigg, R. *Acta Crystallogr. Sect B* **1993**, *49*, 708.
(19) Kohne, B.; Praefcke, K.; Mann, G. *Chimia* **1988**, *42*, 139.
(20) Fattah, J.; Twyman, J. M.; Dobson, C. M. *Magn. Reson. Chem.* **1992**, *30*, 606.
(21) Zamir, S.; Bernstein, J.; Greenwood, D. *J. Mol. Cryst. Liq. Cryst.* **1994**, *242*, 193.
(22) Skoko, Ž.; Zamir, S.; Naumov, P.; Bernstein, J. *J. Am. Chem. Soc.* **2010**, *132*, 14191.
(23) Ding, J.; Herbst, R.; Praefcke, K.; Kohne, B.; Saenger, W. *Acta Crystallogr. Sect B* **1991**, *47*, 739.

(24) Corbett, J. M.; Dickman, M. H. *Acta Crystallogr., Sect. C* **1996**, *52*, 1851.
(25) Davey, R. J.; Maginn, S. J.; Andrews, S. J.; Black, S. N.; Buckley, A. M.; Cottier, D.; Dempsey, P.; Plowman, R.; Rout, J. E.; Stanley, D. R.; Taylor, A. *Mol. Cryst. Liq. Cryst.* **1994**, *242*, 79.
(26) Corbett, J. M.; Dickman, M. H. *Acta Crystallogr., Sect. C* **1996**, *52*, 1851.
(27) Takemura, H. *Chemistry* **2005**, *60*, 46.
(28) Wu, H.; Reeves-McLaren, N.; Pokorny, J.; Yarwood, J.; West, A. R. *Cryst. Growth Des.* **2010**, *10*, 3141.
(29) Al-Kaysi, R. O.; Müller, A. M.; Bardeen, C. J. *J. Am. Chem. Soc.* **2006**, *128*, 15938.
(30) Zhu, L.; Agarwal, A.; Lai, J.; Al-Kaysi, R. O.; Tham, F. S.; Ghaddar, T.; Mueller, L.; Bardeen, C. J. *J. Mater. Chem.* **2011**, *21*, 6258.
(31) Kim, T.; Zhu, L.; Mueller, L. J.; Bardeen, C. J. *CrystEngComm* **2012**, *14*, 7567.
(32) Shtukenberg, A. G.; Freudenthal, J.; Kahr, B. *J. Am. Chem. Soc.* **2010**, *132*, 9341.
(33) Al-Kaysi, R. O.; Bardeen, C. J. *Adv. Mater.* **2007**, *19*, 1276.
(34) Good, J. T.; Burdett, J. J.; Bardeen, C. J. *Small* **2009**, *5*, 2902.
(35) Zhu, L.; Al-Kaysi, R. O.; Bardeen, C. J. *J. Am. Chem. Soc.* **2011**, *133*, 12569.
(36) Naumov, P.; Kowalik, J.; Solntsev, K. M.; Baldridge, A.; Moon, J.-S.; Kranz, C.; Tolbert, L. M. *J. Am. Chem. Soc.* **2010**, *132*, 5845.
(37) Ichimura, K. *Chem. Commun.* **2009**, 1496.
(38) Koshima, H.; Ojima, N.; Uchimoto, H. *J. Am. Chem. Soc.* **2009**, *131*, 6890.
(39) Koshima, H.; Ojima, N. *Dyes Pigments* **2012**, *92*, 798.
(40) Koshima, H.; Takechi, K.; Uchimoto, H.; Shiro, M.; Hashizume, D. *Chem. Commun.* **2011**, *47*, 11423.
(41) Kobatake, S.; Takami, S.; Muto, H.; Ishikawa, T.; Irie, M. *Nature* **2007**, *446*, 778−781.
(42) Morimoto, M.; Irie, M. *J. Am. Chem. Soc.* **2010**, *132*, 14172.
(43) Terao, F.; Morimoto, M.; Irie, M. *Angew. Chem., Int. Ed.* **2012**, *51*, 901.
(44) Uchida, K.; Sukata, S.; Matsuzawa, Y.; Akazawa, M.; de Jong, J. J. D.; Katsonis, N.; Kojima, Y.; Nakamura, S.; Areephong, J.; Meetsma, A.; Feringa, B. L. *Chem. Commun.* **2008**, 326.
(45) Koshima, H.; Nakaya, H.; Uchimoto, H.; Ojima, N. *Chem. Lett.* **2012**, *41*, 107.
(46) Abakumov, G. A.; Nevodchikov, V. I. *Dokl. Akad. Nauk SSSR* **1982**, *266*, 1407.
(47) Lange, C. W.; Foldeaki, M.; Nevodchikov, V. I.; Chekrasov, V. I.; Abakumov, G. A.; Pierpont, C. G. *J. Am. Chem. Soc.* **1992**, *114*, 4220.
(48) Boldyreva, E. V.; Sidelnikov, A. A.; Chupakhin, A. P.; Lyakhov, N. Z.; Boldyrev, V. V. *Proc. Acad. Sci. USSR* **1984**, *277*, 893.
(49) Boldyreva, E. V.; Sidel'nikov, A. A. *Proc. Sib. Dept. Acad. Sci. USSR* **1987**, *5*, 139.
(50) Yakobson, B. I.; Boldyreva, E. V.; Sidel'nikov, A. A. *Proc. Sib. Dept. Acad. Sci. USSR* **1989**, *51*, 6.
(51) Boldyreva, E. V.; Burgina, E. B.; Baltakhinov, V. P.; Burleva, L. P.; Ahsbahs, H.; Uchtmann, H.; Dulepov, V. E. *Ber. Bunsen. Phys. Chem.* **1992**, *96*, 931.
(52) Boldyreva, E. V.; Podberezskaya, N. V.; Virovets, A. V.; Burleva, L. P.; Dulepov, V. E. *J. Struct. Chem.* **1993**, *34*, 128.
(53) Wu, H.; West, A. *Cryst. Growth Des.* **2011**, *11*, 3366.
(54) Boldyreva, E. V.; Drebushchak, V. A.; Drebushchak, T. N.; Paukov, I. E.; Kovalevskaya, Yu. A.; Shutova, E. S. *J. Therm. Anal. Calorim.* **2003**, *73*, 419.
(55) Minkov, V. S.; Drebushchak, V. A.; Ogienko, A. G.; Boldyreva, E. V. *CrystEngComm* **2011**, *13*, 4417.
(56) Boldyreva, E. V.; Drebushchak, V. A.; Paukov, I. E.; Kovalevskaya, Yu, A.; Drebushchak, T. N. *J. Therm. Anal. Calorim.* **2004**, *77*, 607.
(57) Grinfeld, M. A. *Dokl. Akad. Nauk SSSR* **1986**, *290*, 1358.
(58) Gelbrich, T.; Hursthouse, M. B. *CrystEngComm* **2005**, *7*, 324.
(59) Gelbrich, T.; Hursthouse, M. B. *CrystEngComm* **2006**, *8*, 448.
(60) van Zoeren, E.; Oonk, H. A.; Kroon, J. *Acta Crystallogr. Sect B* **1978**, *34*, 1898.
(61) Crottaz, O.; Kubel, F.; Schmid, H. *J. Mater. Chem.* **1997**, *7*, 143.
(62) Bertaut, F.; Delorme, C. C. R. *Acad. Sci (Paris)* **1954**, *239*, 505.
(63) Prince, E. *J. Appl. Phys.* **1961**, *32*, 68.
(64) PHA might appear as an exception from this rule; however, note that the reported structure of the (red) HT phase β (Table 2) does not correspond to the structure (γ) that evolves during the TS transition ($\alpha \rightarrow \gamma$). Therefore, a direct comparison of phase α with the HT phase β is not possible.
(65) As shown in Table 2, the cells of the only two known inorganic TS crystals (spinel structures) expand strongly (38.7−42.5%) and the crystal symmetry changes from tetragonal to cubic. Due to the different mechanism of the transition in this case (Jahn−Teller effect) and the different nature of bonding in these two structures, they were excluded from the discussion.
(66) Basic crystallographic data: $C_{10}H_{12}N_2O_2$, M_r = 192.22, monoclinic, $P2_1/c$, a = 7.6315(11) Å, b = 12.0996(17) Å, c = 10.2473(14) Å, β = 97.950(2)°, V = 937.1(2) Å^3, Z = 4, Final R indices [$I > 2\sigma(I)$], R_1 = 0.0409, wR_2 = 0.1178; R indices (all data), R_1 = 0.0484, wR_2 = 0.1290.
(67) Fábián, L.; Kálmán, A. *Acta Crystallogr., Sect. B* **2004**, *60*, 547.
(68) Fabbiani, F. P. A.; Dittrich, B.; Florence, A. J.; Gelbrich, T.; Hursthouse, M. B.; Kuhs, W. F.; Shankland, N.; Sowa, H. *CrystEngComm* **2009**, *11*, 1396.
(69) Kálmán, A.; Párkányi, L.; Argay, G. *Acta. Crystallogr., Sect B* **1993**, *49*, 1039.
(70) Smallman, R. E. *Modern Physical Metallurgy*, 3rd ed.; Butterworth: London, 1970.
(71) Cahn, R. W. *Physical Metallurgy*; Cahn, R. W., Haasen, P., Eds.; Elsevier, 1996.
(72) Kurdyumov, G. V. *Metalloved. Term. Obrab. Met.* **1997**, *2*, 31.
(73) Roitburd, A. L. *Mater. Sci. Eng., A* **1990**, *127*, 229.
(74) Roitburd, A. L. *Bull. Acad. Sci. U.S.S.R.* **1982**, *47*, 17.
(75) Roitburd, A. L.; Kurdjumov, G. V. *Mater. Sci. Eng.* **1979**, *39*, 141.
(76) Roitburd, A. L. *Solid State Phys.* **1978**, *33*, 317.
(77) Roitburd, A. L. *Phys. Status Solidi A* **1977**, *40*, 333.